6-1996

Charge collection and trapping in low-temperature silicon detectors

M. J. Penn

Brian L. Dougherty

Blas Cabrera

R. M. Clarke

Betty A. Young
Santa Clara University, byoung@scu.edu

Recommended Citation

Penn, M. J., Dougherty, B. L., Cabrera, B., Clarke, R. M., & Young, B. A. (1996). Charge collection and trapping in low-temperature silicon detectors. Journal of Applied Physics, 79(11), 8179–8186. https://doi.org/10.1063/1.362552

Charge collection and trapping in low-temperature silicon detectors

M. J. Penn,[a] B. L. Dougherty,[b] B. Cabrera, and R. M. Clarke
Department of Physics, Stanford University, Stanford, California 94305-4060

B. A. Young
Department of Physics, Santa Clara University, Santa Clara, California 95053

(Received 28 December 1995; accepted for publication 29 February 1996)

Charge collection efficiency measurements in silicon detectors at low temperature ($T<0.5$ K) and low applied electric field ($E=0.1-100$ V/cm) were performed using a variety of high-purity, p-type silicon samples with room-temperature resistivity in the range 2–40 kΩ cm. Good charge collection under these conditions of low temperature and low electric field is necessary for background suppression, through the simultaneous measurement of phonons and ionization, in a very low event rate dark matter search or neutrino physics experiment. Charge loss due to trapping during drift is present in some samples, but the data suggest that another charge–loss mechanism is also important. We present results which indicate that, for 60 keV energy depositions, a significant fraction of the total charge loss by trapping occurs in the initial electron-hole cloud near the event location which may briefly act as a shielded, field-free region. In addition, measurements of the lateral size, transverse to the applied electric field, of the initial electron-hole cloud indicate large transverse diffusion lengths. At the lowest fields a lateral diameter on the order of 1 mm is found in a detector ~5 mm thick. © *1996 American Institute of Physics.* [S0021-8979(96)08311-9]

I. INTRODUCTION

Particle interactions in a silicon detector excite both phonons and electron-hole pairs. Phonons may be detected passively through the use of bolometers or other sensors on the crystal surface,[1] whereas an electric field is required to separate and drift the charge carriers. The nuclear-recoil/electron-recoil discrimination technique (based on the simultaneous measurement of phonons and ionization)[2] that we are developing for a dark matter search requires reasonably good (~90%) charge collection efficiency. However, electric-field strengths must be kept low in order to minimize the extra charge-drift induced phonon energy which contaminates the initial phonon signal arising from the event.[3] Our cryogenic dark matter search (CDMS) experiment will use detector substrates that are about 1 cm thick, and we need to be able to achieve good charge collection with only ~few V/cm applied electric field. Unfortunately, charge collection efficiency drops rapidly at very low applied field, presumably due to charge trapping (see Fig. 1).

A number of high-purity silicon detectors were studied in order to analyze the low-field trapping effects and their dependence on crystal purity and thickness. A simple model of charge trapping during drift fails to account for the detector thickness dependence of the trapping seen in the data. By including enhanced trapping effects in the initial, field-free electron-hole plasma, satisfactory comparison to the data is found.

II. ELECTRON STOPPING IN Si

When a photon with energy of order 10 keV is photoabsorbed by an electron in a semiconductor like silicon, that electron excites a large number of other electron-hole pairs as it rapidly slows down. The initial energy is subsequently divided among several generations of electron-hole pairs until the energies of these excited free charge carriers fall below the threshold for further ionization production. Below this threshold, the charges continue to "cool" to the band edges by phonon emission. At a threshold of ~0.2 meV (~2 K equivalent temperature), corresponding to a velocity equal to the speed of sound in silicon, the charges can no longer emit or absorb phonons.[4] In a field-free detector at $T<2$ K the electrons and holes will presumably diffuse against impurities after reaching this threshold. In very-high-purity silicon, the elastic scattering length for neutral impurities can be as large ~100 μm, so charges can perhaps diffuse macroscopic distances before reaching the crystal temperature.

For 60 keV depositions in silicon at $T\sim2$ K, the average total track length for the initial photoelectron is ~35 μm.[5] The secondary electrons and holes have energies ~100 eV[5] and they will initially thermalize to ~2 K after moving ~10 nm.[6] The average energy spent to create an electron-hole pair is $\approx$3.7 eV.[7] If the resulting electron-hole cloud is considered roughly spherical with radius ~15 μm then the charge density is $n\sim10^{12}$ electron-hole pairs cm^{-3}. This density is roughly independent of deposited energy since for smaller energy depositions fewer charges will be found in a smaller volume. At low temperatures, this electron-hole cloud is dense enough to be considered a plasma since the Debye shielding length ($\lambda_D=740(\kappa T_{eV}/n)^{1/2}$ cm$\approx$0.3 μm at 2 K[8] where T_{eV} is the temperature in eV, κ is the dielectric constant of silicon, and n is the charge density in cm^{-3}) is much smaller than the size of the cloud. It is likely, therefore, that the interior of the cloud is shielded from an applied electric field. Such shielding is temporary since the cloud will expand by diffusion and will be eroded from its surface by the electric field.

[a]Electronic mail: mjpenn@leland.stanford.edu
[b]Current address: Jet Propulsion Laboratory, MS169-327, 4800 Oak Grove Dr., Pasadena, CA 91109.

 0021-8979/96/79(11)/8179/8/$10.00

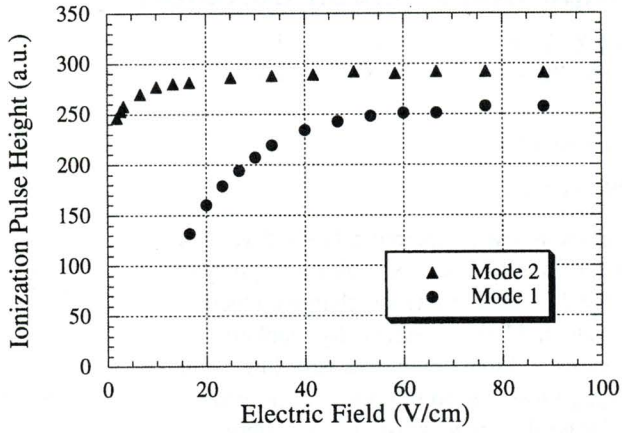

FIG. 1. Typical 60 keV ionization pulse height vs electric field data for Mode 1 and Mode 2 in a 300-μm-thick detector. Charge collection efficiency is better at low field for Mode 2 compared to Mode 1.

Once "caught" in the applied field, electrons and holes drift in opposite directions and induce charge signals in the corresponding electrodes. The charge collection efficiency depends on the strength of the electric field. In Fig. 1 we plot the position of the 60 keV peak in the ionization pulse height spectrum as a function of electric field. We suppose that the dominant charge loss mechanism is trapping on impurities in the initial cloud or during drift. Electron-hole recombination during drift should be negligible since the different sign charges are drifting away from each other. Recombination within the initial cloud is also expected to be negligible in our high-purity samples since Auger recombination is suppressed at low carrier density,[9] and recombination through trapping sites is reduced by the lack of strong trapping centers in the samples under our experimental conditions (see Sec. III, below). It should be emphasized, however, that although charge loss in the cloud due to recombination seems unlikely, it is essentially indistinguishable experimentally from simple trapping.

III. EQUILIBRIUM CONDITIONS IN A SEMICONDUCTOR CRYSTAL AT LOW TEMPERATURE

The equilibrium state of a semiconductor is given by the condition of charge neutrality. In all the experiments described here p-type silicon was used. Thus, $N_A > N_D$ where N_A is the density of acceptor impurities and N_D is the density of compensating donor impurities. At low temperature ($T<1$ K), there will be no thermally generated free carriers since the energy required to excite free charge from dopant impurities ($\sim$30 meV) is much larger than the available thermal energy ($k_B T<100$ μeV), and we can visualize the state of the crystal in a simple way. (There is certainly not any free charge excited across the gap since $E_{\text{gap}} \approx 1.2$ eV is even larger than the energy required to ionize a dopant impurity.)

A simple, qualitative way to determine the state of the crystal relies on the observation that it is energetically favorable for each donor impurity to give up its electron to a nearby acceptor. Both impurities are left ionized: the donor is empty (D^+) and the acceptor is occupied (A^-). At low temperature, these ionized impurities form dipole pairs between a donor and the nearest acceptor.[10] Thus, in the thermal equilibrium state of a p-type semiconductor at very low temperature all compensating donors are ionized (empty) as are an equal number of acceptors (occupied). The majority of acceptors, $N_A - N_D$ per cm^3, remain neutral, since the crystal must be electrically neutral overall, and there are no thermally generated free charge carriers.

This picture of the crystal is modified after prolonged exposure to ionizing radiation. Our detectors operate in two distinct modes which differ in the number of ionized impurities which contribute to charge trapping mechanisms.[11] Just after cooldown, the detector is found to operate in Mode 1, which corresponds to the thermal equilibrium state described above. Here we have N_D ionized donors and acceptors per cm^3. When particle interactions excite free electron-hole pairs, each carrier can trap on the ionized impurity of opposite sign, leaving that impurity electrically neutral. At our operating temperature these trapped charges are not reemitted. The ionized impurities act as both elastic scattering sites and traps. For $N_D = 3\times10^{12}$ cm^{-3} (a typical value for the silicon used in our experiments), and after free charges have cooled to the band edges, the elastic scattering length is $\sim$0.3 μm (elastic scattering cross section $\sim10^{-8}$ cm^2)[12] and the trapping cross section is $\sim10^{-11}$ cm^2.[10] Under field-free conditions, the thermalized free charges become trapped on ionized impurities after diffusing an average distance of ~5 μm from the location where they thermalized. This trapping is a serious impediment to charge collection at low electric field.

As the detector is exposed to ionizing radiation for a prolonged period (of order hours in our experiments), the ionized impurities become gradually neutralized. Then, we no longer have a thermal equilibrium state described by a Fermi level; instead, the crystal attains a long lived metastable state which we call Mode 2. Once in Mode 2, the detector remains stable (no reemission of trapped charge) for more than two weeks (our longest run), provided that the detector is kept below $T\sim12$ K. Scattering and trapping are then dominated by neutral impurity processes for which cross sections are orders of magnitude smaller ($\sim10^{-10}$ cm^2 for elastic scattering[12] and $\sim10^{-13}$ cm^2 for trapping[13]) and event-induced free charges can diffuse through the crystal and reach the surfaces. Since the density of neutral impurities is of order $N_A\sim10^{13}$ cm^{-3} for our silicon, the elastic scattering length is ~10 μm and the trapping length is ~1 cm. The charges can diffuse ~200 μm before trapping. In Mode 2, charge loss due to trapping is much reduced and, in general, detector performance is greatly improved (see Fig. 1). All the data presented here were taken with the detectors operating in Mode 2, which is of most interest for detector applications.

IV. SIMPLE TRAPPING MODEL

The simplest model of charge loss in our detectors includes only trapping along the drift path. All of the free electrons and holes excited by a particle interaction start at a common point in the crystal and then drift to opposite elec-

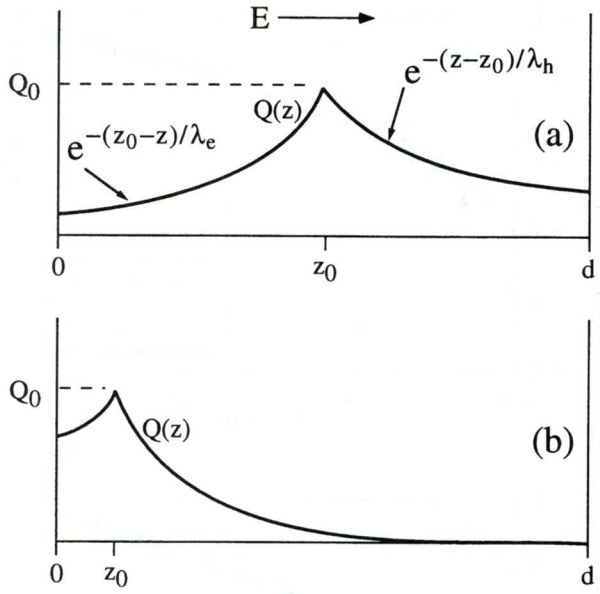

FIG. 2. Behavior of simple trapping model. Electrons and holes drift through the detector under the influence of the electric field. A uniform density of traps causes exponential attenuation of the drifting charge. The measured signal is the area under the curves for (a) an event near the center of the detector, or (b) an event near one side of the crystal. The largest signal is for events which occur near the center of the detector.

trodes with constant drift velocity. This model assumes that the charges are very quickly accelerated to their drift velocities. The charges trap on a uniform density of impurities and each charge has the same chance to trap per unit drift length. The drifting charge is therefore attenuated exponentially with drift distance z

$$Q(z)=Q_0 e^{-z/\lambda}, \tag{1}$$

where Q_0 is the initial number of charges created in the event. It is expected that the trapping length should scale as $\lambda \sim 1/\sigma N_A$, with the trapping cross section σ decreasing for increasing applied electric field.

If an amount Q of charge drifts a distance dz between parallel electrodes then, by Ramo's theorem,[14] signal charge is induced on the electrodes of amount

$$dS=Q\,\frac{dz}{d}, \tag{2}$$

where d is the thickness of the detector and dS represents the signal charge. If Q_0 is deposited at position z_0 then Eq. (1) allows us to plot Q as a function of z, as in Fig. 2(a). In Fig. 2, the electrons drift against the direction of the electric field with trapping length $\lambda_e(E)$ and the holes drift along the field with trapping length $\lambda_h(E)$. The total signal will be given by the area under the curve, i.e., the integral of $Q(z)$ over z. Figure 2(b) demonstrates (with $\lambda_h \approx \lambda_e$) that for events near the edges of the detector the signal is smaller. For ionizing events generated uniformly throughout the crystal ($1/e$ attenuation length for 60 keV photons in Si is $\sim$3 cm), and $\lambda_h \approx \lambda_e$, the maximum signal occurs at $z_0 \approx d/2$. Carrying out the integrals, and defining a mean trapping length $2\lambda(E) \equiv \lambda_e(E)+\lambda_h(E)$, we obtain a prediction for the maximum charge collection efficiency (normalized pulse height, $\mathrm{PH}=S_{\max}/Q_0$) as a function of electric field

$$\mathrm{PH}=\frac{2\lambda(E)}{d}\,(1-e^{-d/2\lambda(E)}). \tag{3}$$

Two general statements can be made with respect to Eq. (3). First, as the electric field is increased the trapping length is presumed to rise and therefore the signal increases. At large enough electric field the pulse height saturates and becomes independent of applied field. Since it is expected that λ also rises with decreasing N_A, a crystal with N_A as small as possible (highest purity) is desirable. Second, Eq. (3) indicates that for any particular λ (i.e., N_A and σ), a detector which is thicker (d larger) will give smaller signals. Thus, we have an explicit prediction for how the pulse height should depend on detector thickness for detectors made from nominally the same starting material.

V. EXPERIMENTAL SURVEY OF Si SAMPLES

A variety of high-purity, p-type, $\langle 100 \rangle$ silicon samples were studied for charge collection at low electric field and low temperature. The samples are about 1 cm$\times$1 cm and vary in thickness from 300 μm to nearly 5 mm. Thin ($\sim$40 nm thick) Ti electrodes were deposited on the top and bottom faces of the samples. For each of the three highest purity samples (with room temperature resistivity of 8, 15, and 40 kΩ cm) two different thicknesses were fabricated from the same bulk material, typically $\sim$2 and $\sim$5 mm. For the lowest purity samples (with room-temperature resistivity of 2 kΩ cm) three thicknesses were examined: 300 μm, 1 and 2 mm. All the crystals were grown specifically for high purity, either by magnetic-Czochralski or float-zone techniques. The high resistivity of the samples is, therefore, not achieved by intentional compensation. For the 2 kΩ cm samples $N_A \sim 10^{13}$ cm^{-3} and for the higher resistivity samples $N_A \sim 10^{12}$ cm^{-3}.

The detectors were characterized by exposure to electron-recoil energies of 60 and 25 keV. The results were virtually identical for these two energies and in what follows only the 60 keV data will be discussed. Our experiments consisted of measuring relative ionization pulse height in Mode 2 at different applied electric fields. It was not possible in the thicker samples ($d>2$ mm) to apply a large enough electric field to saturate the pulse height. In other words, we could not reach the flat, asymptotic region of pulse height versus electric field shown for a thin sample in Fig. 1. Pulse heights were therefore normalized to an extrapolated maximum signal by fitting the data to a smooth curve. This procedure, in which all data sets were treated equally, introduces a common-mode uncertainty in the normalized pulse height values of $\sim$20% depending on how the extrapolation is done. This common-mode uncertainty does not affect any of the conclusions drawn from the relative positions of the various data sets. Each data point in the sets has a relative uncertainty of $\sim$3%.

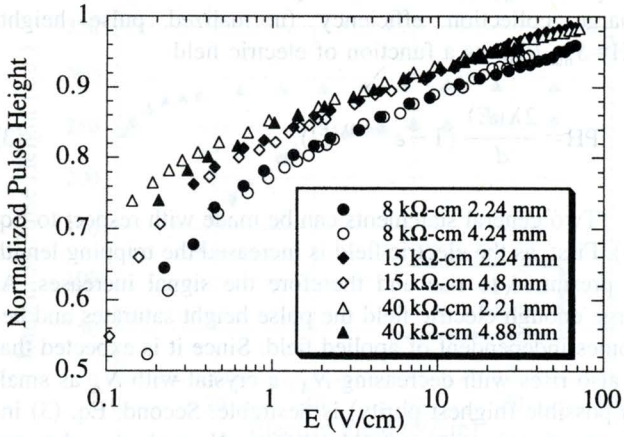

FIG. 3. Normalized pulse height vs electric field for high-purity samples.

A. Review of charge collection data

Data for the three highest purity samples are presented together in Fig. 3. The general trend of better charge collection for the higher purity samples is seen. For clarity the data are also presented separately in Fig. 4(a)–4(c) along with solid curves which will be discussed in Sec. VI. Most notable in Fig. 4(a)–4(c) is a complete lack of thickness dependence for each of the three purities. In stark contrast to Eq. (3) the data show that the charge collection efficiency is the same for detectors ~2 mm thick and ~5 mm thick.

Data for the lowest purity samples (2 kΩ cm) are shown in Fig. 5. Here there is a clear thickness dependence with the thicker detectors giving lower charge signal at the same electric field. Each data point (normalized pulse height $PH=S_{max}/Q_0$) in the topmost data set in Fig. 5 can be converted into a $\lambda(E)$ using Eq. (3). The simple trapping model predicts that the deduced $\lambda(E)$ will be the same for all three thicknesses. This can be tested by taking the 300 μm results and recalculating via Eq. (3), but using $d=1$ mm and $d=2$ mm. The predictions are shown as dashed lines in Fig. 5. Once again we find that the simple trapping model does not explain the data. In this case the data do show some thickness dependence but to a lesser degree than that predicted by Eq. (3).

B. Charge coincidence experiments

The inability of the simple trapping model to account for the lack of thickness dependence of the data leads us to suppose that much of the charge loss could be occurring in a small region close to the interaction location. Since this "source region" is smaller than the detector thickness, the charge collection efficiency should not depend on thickness. On the other hand, if the charge loss is partially in the source region (same for all thicknesses) and partially along the drift (more for thicker detectors), then the data will behave roughly as shown in Fig. 5. We suppose that the source region is the initial electron-hole cloud which is formed by a particle interaction.

In order to measure the size of this cloud, we instrumented a detector (40 kΩ cm, 4.88 mm thick) with one elec-

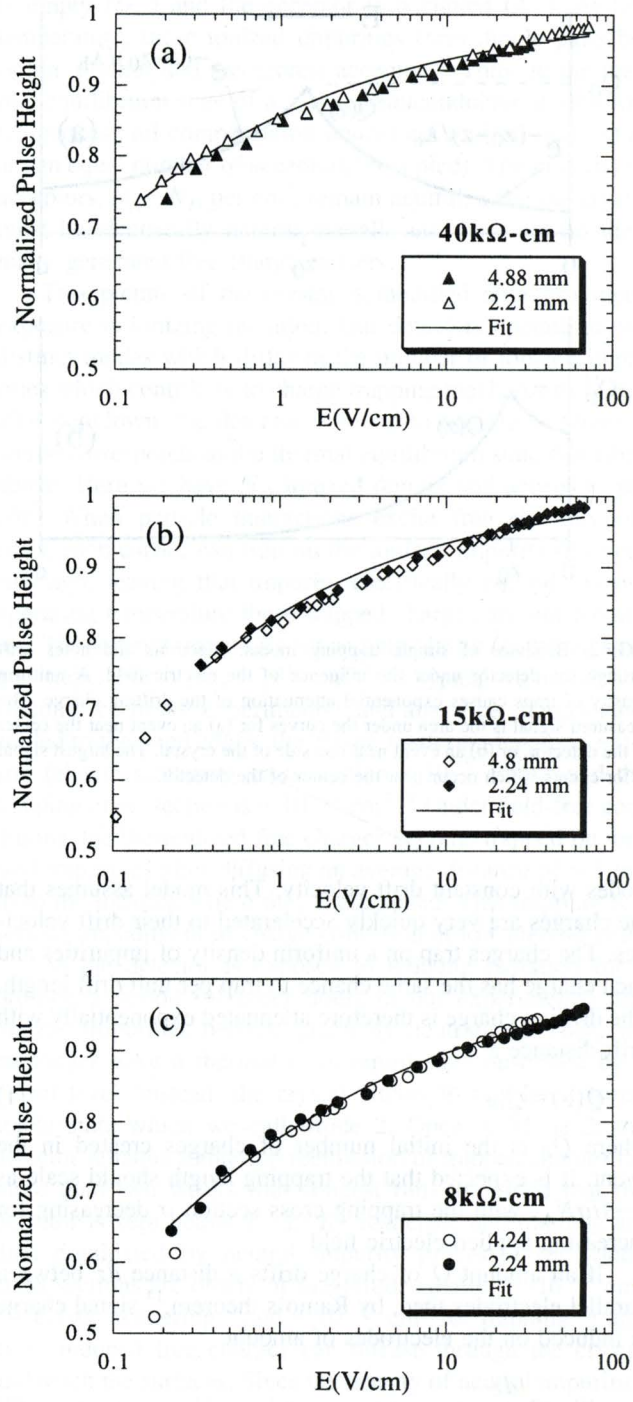

FIG. 4. Normalized pulse height vs electric field for high-purity samples with fit to model described in Sec. VI: (a) 40 kΩ cm samples, (b) 15 kΩ cm samples, and (c) 8 kΩ cm samples.

trode split in half as shown in Fig. 6(a). The top electrodes are now each about 1 cm×5 mm, with ≈0.3 mm gap between them. We picture the cloud as expanding to some radius before being pulled apart by the electric field. In our setup, then, we can correlate the size of the cloud transverse to the electric field to the partitioning of the charge signal between the two electrodes. If the cloud is idealized as a sphere of radius $a(E)$ with uniform charge density, then the split-electrode detector will see coincident pulses only if the

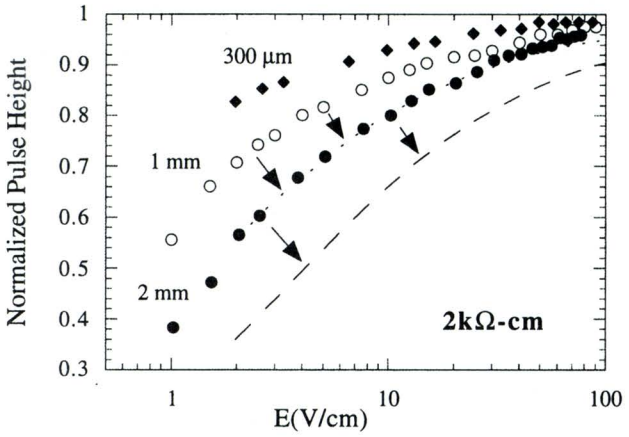

FIG. 5. Normalized pulse height data for 2 kΩ cm samples showing predictions of the simple trapping model. Dashed lines indicate where 1 and 2 mm data would lie (relative to the 300 μm data) if trapping only occurred during drift.

event occurs within a distance $a(E)$ of the split [see Figs. 6(b) and 6(c)]. Otherwise, only one electrode will collect a signal. A cut can be made on the data to insure that a total of 60 keV of energy is collected [horizontal dashed lines in Fig. 6(c)]. The ratio, R, of the rate of coincident pulses to the rate of single pulses, for uniform illumination of the detector with 60 keV photons, is therefore

$$R=\frac{2a(E)}{w-2a(E)} \tag{4}$$

with w=detector width. This expression can be rewritten to extract $a(E)$

$$2a(E)=w\,\frac{R}{1+R}. \tag{5}$$

Since the cloud is not exactly spherical with uniform density we should use Eq. (5) as a rough guide only.

Data were collected with the split electrode configuration at different electric fields and the rate of coincidences was found to rise with decreasing applied field. The results are shown in Fig. 7. The statistics in the experiment are poor and the error bars shown in Fig. 7 are entirely statistical. A two parameter fit to the data is also shown in Fig. 7. The fit indicates that $2a(E)=(1.4\pm0.05)E^{(-0.19\pm0.03)}$ mm for E measured in units of V/cm. Thus, the data indicate that a large, $\approx$1 mm charge cloud is present at low electric fields. The scale of this cloud is much larger than the track length of the initial photoelectron ($\sim$35 μm). We suspect that this large cloud size is due to the threshold for phonon emission at energy $\sim$0.2 meV. After slowing to below this energy, the electrons diffuse against impurities and can quickly reach macroscopic distances in high-purity crystals.

Accidental coincidences could occur, giving a field-independent rate, if a 60 keV photon Compton scatters in one half of the detector and then is photoabsorbed in the other half. The detector would, in this case, still measure a total (summed) pulse height of 60 keV. An estimate of the rate of such contaminating events contributes negligibly to the error bars in Fig. 7. In addition, R could be affected by drift induced transverse spreading of the charges. This effect, which is calculated[15] to be nearly independent of applied electric field, is found to give a coincidence rate at least a factor of 4 lower than what we measured at the highest fields.

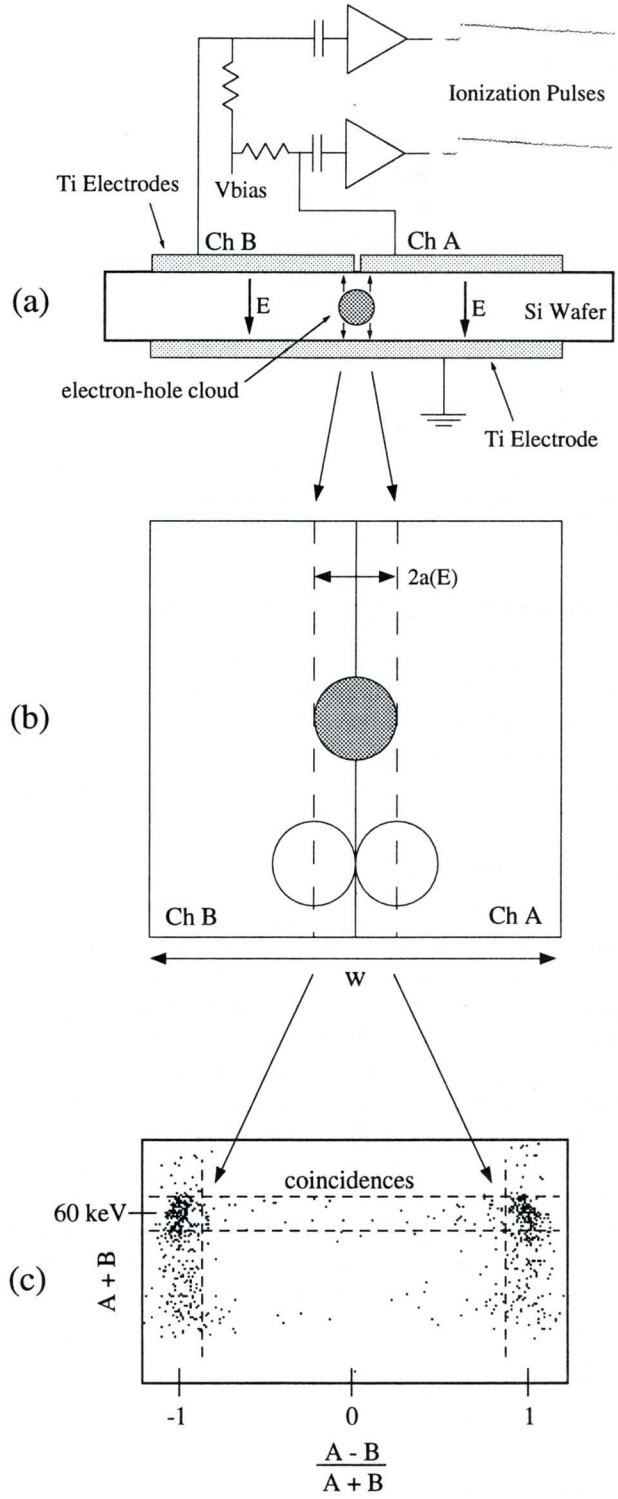

FIG. 6. Schematic diagram of detector for the simultaneous ionization experiment: (a) the top electrode is split into two channels (A and B) in order to measure the lateral size of the electron-hole cloud, (b) expanded view from above, (c) data is plotted as (A−B)/(A+B), where A and B represent the charge signal in the two channels, and events which lie within the horizontal (60 keV total signal) and vertical (threshold for coincidence) dashed lines are shared by two channels.

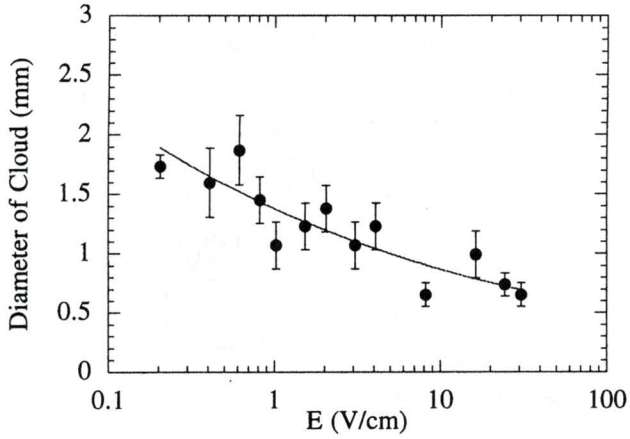

FIG. 7. Rate of coincident ionization pulses converted to cloud diameter using Eq. (5). The smooth curve is a two parameter fit, diameter$=bE^{-c}$ mm where $b=1.4$ and $c=0.19$.

VI. ANALYSIS OF CHARGE COLLECTION DATA

The simple trapping model presented in Sec. IV fails to explain the thickness dependence of the data in every sample. In addition, we have experimental evidence which suggests that a macroscopic charge cloud is present at low electric field which could be influencing the charge measurements.

A. High-purity samples

The data in Figs. 4(a)–4(c) show no thickness dependence at all. This implies that all of the charge loss is occurring in the initial cloud with no further loss due to trapping during drift after the electric field penetrates the cloud. The simplest model of this situation is one of charge diffusion and trapping in a field-free region near the event location which is shielded temporarily from the applied electric field by the electron-hole plasma. Each charge carrier executes a random walk in three dimensions, independent of the others, with a constant step length (λ_{step}) and a constant trapping length (λ_{trap}), both of which are determined by the relevant cross sections and the density of impurities. Let $n(r)$ be the relative density of charge carriers. Simple diffusion theory implies

$$\nabla^2 n = n/L^2, \tag{6a}$$

where $L^2=\lambda_{step}\lambda_{trap}/3$.[16] Thus,

$$n(r)=\frac{e^{-r/L}}{2\pi r L^2}. \tag{6b}$$

Since capture probability is proportional to carrier density, we may treat $n(r)$ as the distribution of trapped charge. The fraction of carriers which survive beyond radius a is then

$$\frac{Q}{Q_0}=\left(1+\frac{a}{L}\right)e^{-a/L}. \tag{7}$$

We assume this radius a approximates the maximum cloud radius attained before complete erosion by the electric field.

Thus we have a very simple model of charges diffusing in the cloud, some fraction of them trapping in the process, before the remainder are drifted to the detector electrodes without further attenuation. This model clearly does not contain the actual dynamics of the situation, which include erosion of the cloud from its surface as it expands and the fact that a larger fraction of the charges in the cloud are affected by the electric field as its density decreases with expansion (λ_D increases and shielding is less effective). In addition, the actual step and trapping lengths will not be constants and the electrons and holes will need to be treated separately. As a simple, zeroeth-order model, however, it contains the necessary features which are required by the data: a plausible mechanism by which the interior of the cloud is temporarily shielded from the electric field, and a means by which charges can trap before leaving the cloud.

TABLE I. Parameters used in the charge cloud model fit to Eq. (7) shown as solid lines in Figs. 4(a)–(c).

Sample	$\frac{b}{L}$	n
40 kΩ cm	0.658±0.006	0.21±0.01
15 kΩ cm	0.730±0.01	0.24±0.01
8 kΩ cm	0.887±0.006	0.21±0.01

In order to estimate how the maximum cloud radius could depend on applied electric field, we can consider the problem of a conducting, metal sphere in a uniform electric field. The total amount of charge available for shielding is spread over a sphere of radius a and it cancels the applied field within the sphere. The charge is held on the sphere by the work function of the metal. The amount of charge of each sign required to shield an applied field E_a is $Q\sim E_a a^2$. Thus, for a given amount of available charge created in an event, a will scale as $E_a^{-1/2}$. The electron-hole cloud is not a conducting sphere, however, since the charges diffuse away from each other and since it is pulled apart by the applied field. If λ_{step} is quite small, then the plasma is more strongly confined at early times near the event location and its behavior will more closely resemble the conducting sphere; for λ_{step} larger, the plasma will behave less like a conducting sphere at early times.

The data for the highest purity samples are shown, with fits to Eq. (7), in Fig. 4(a)–4(c). In these fits we set $a(E)=bE^{-n}$ and fit to the parameters b/L and n. The results are shown in Table I. Remarkably, the fits require $a(E)\sim E^{-0.2}$, the same result found in our coincident charge measurements. Also, the coincident charge measurements give an independent measure of the parameter b for the 40 kΩ cm sample, namely $b\approx 0.07$ cm. This allows us to estimate the values of λ_{step} and λ_{trap} in these detectors. Since $b/L\approx 0.66$ and $a\approx 0.07$ cm we get $\lambda_{step}\lambda_{trap}\sim 0.03$ cm^2. These numbers are consistent with order of magnitude estimates from the cross sections and impurity density ($N_A\sim 10^{12}$ cm^{-3}, $\sigma\sim 10^{-10}$ cm^2 for elastic scattering, and $\sigma\sim 10^{-13}$ cm^2 for trapping),[12,13] which give $\lambda_{step}\sim 0.01$ cm and $\lambda_{trap}\sim 10$ cm. The parameter b/L is slightly higher in the 15 kΩ cm and 8 kΩ cm detectors indicating a higher impurity density which will make λ_{step} and λ_{trap} smaller.

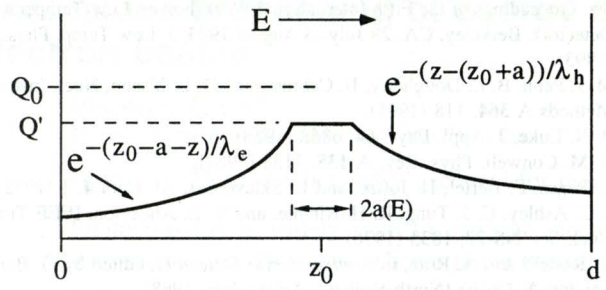

FIG. 8. Hybrid trapping model. Electron-hole cloud of radius $a(E)$ shields its interior from the applied electric field. A fraction Q' of the charge generated in an event does not trap in the cloud and it drifts to the electrodes. The trapping during drift is expressed by the exponentials. The measured signal is the area under the curve.

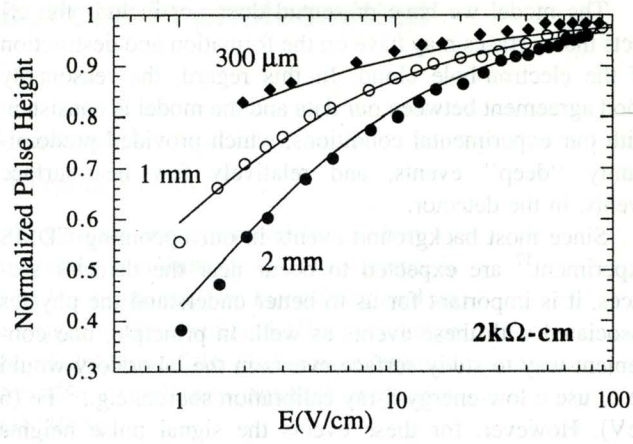

FIG. 9. Normalized pulse height vs electric field for the 2 kΩ cm samples showing the fit to Eq. (8). The parameters of the fit are given in Table II.

B. 2 kΩ cm samples

For the 2 kΩ cm samples we need a hybrid model which includes charge loss in the cloud plus loss during drift (see Fig. 5). This is a straightforward extension of the simple trapping model of Sec. 4. Figure 8, in analogy to Fig. 2, shows the situation. The charge which survives the cloud is separated by the diameter of the cloud. No signal is derived from within the cloud since both electrons and holes are presumed to diffuse uniformly and only a net separation of charge gives signal. The problem is reduced to one dimension and the fact that the cloud is at least roughly spherical is neglected: all the surviving charge is assumed to separate to the diameter of the cloud. Following Sec. IV, the total signal is given by the area under the curve shown in Fig. 8. Again, defining the mean trapping length $2\lambda(E)\equiv\lambda_e(E)+\lambda_h(E)$, and computing the area under the curve in Fig. 8 we arrive at this final expression of the model for maximum pulse height as a function of applied field and detector thickness

$$\mathrm{PH}=\left(1+\frac{a(E)}{L}\right)e^{-a(E)/L}\left\{\frac{2a(E)}{d}+\frac{2\lambda(E)}{d}\left(1-e^{-[d-2a(E)]/2\lambda(E)}\right)\right\}. \tag{8}$$

The pre-factor outside the brackets represents the charge loss in the diffuse cloud [Eq. (7)]. The first term in the brackets is the signal from the surviving charge separated to the diameter of the cloud and the second term in the brackets represents the signal due to drifting charge accompanied by trapping [compare to Eq. (3)].

This model requires a five parameter fit to the data for each detector thickness: to find $a(E)=bE^{-n}$ cm, $\lambda(E)=cE^{m}$ cm, and b/L we need to specify five parameters. The set of these five parameters which fit the data for all three thicknesses is given in Table II. The estimated uncertainties listed in Table II were found by varying each parameter in the fit separately. The fits from Eq. (8), using the parameters in Table II, are shown in Fig. 9 for the 2 kΩ cm samples.

In these samples the impurity density is $N_A\sim10^{13}$ cm^{-3}. From this density we can estimate $\lambda_{\mathrm{step}}\sim10$ μm and $\lambda_{\mathrm{trap}}\sim1$ cm. The fit implies that $b\approx0.01$ cm and $n\approx0.3$. (Note that b is smaller than in the higher purity samples, in agreement with the expectation that the charge cloud will not be able to expand as much in the lower purity samples. Also, $n\approx0.3$ is consistent with the more confined plasma behaving more like a conducting sphere compared to the higher purity samples where $n\approx0.2$.) If $b/L\approx0.9$ then $\lambda_{\mathrm{step}}\lambda_{\mathrm{trap}}\approx0.0004$ cm^2, which is consistent with our rough estimates above. The fit also gives us $\lambda(E)\approx0.055E^{0.8}$ cm for E in V/cm. This nearly linear dependence on electric field is reasonable since the applied electric field is analogous to a raised temperature ($T\sim E$) for the drifting electrons and holes. The trapping cross section falls as T^{-1} in a very cold crystal (no phonon induced detrapping)[10] so, by analogy, the trapping length should scale as $\lambda\sim E$.

VII. CONCLUSIONS

Our results on charge collection in high-purity Si crystals at low temperature and low electric field indicate that some amount of the charge loss at low electric field occurs in the initial electron-hole plasma created by a particle interaction. We have presented a simple mathematical model of this loss, and satisfactory comparison to the data was obtained, including rough correspondence with crystal purity differences. In addition we have seen that a simple trapping model which ignores the presence of the cloud is unsatisfactory.

TABLE II. Parameters used in hybrid trapping model fit to Eq. (8) shown as solid lines in Fig. 9.

Sample	$\frac{b}{L}$	b	n	c	m
2 kΩ cm	0.90±0.05	0.010±0.005	0.30±0.02	0.055±0.005	0.80±0.03

The model we have presented does not include the effects that surfaces may have on the formation and destruction of the electron-hole cloud. In this regard, the reasonably good agreement between our data and the model is consistent with our experimental conditions, which provided predominantly "deep" events, and relatively few near-surface events, in the detector.

Since most background events in our upcoming CDMS experiment[17] are expected to occur near the detector surfaces, it is important for us to better understand the physics associated with these events as well. In principle, one convenient way to study surface events in the laboratory would be to use a low-energy x-ray calibration source, e.g., ^{55}Fe (6 keV). However, for these events the signal pulse heights might be uncomfortably close to the electronics noise threshold. Thus, perhaps a better approach would be to irradiate a detector with ~50 keV electrons. This would still provide near-surface electron-recoil events (~10 μm range) but would also give substantial signal pulse heights.

ACKNOWLEDGMENTS

The authors would like to thank W. Tompkins, B. Jones, and D. Sisson for assistance in the experiments. This research was supported in part by DOE Grant No. DE-FG03-90ER40569.

[1] See Proceedings of the Fifth International Workshop on Low-Temperature Detectors, Berkeley, CA, 29 July–3 August 1993, J. Low Temp. Phys. **93** (1993).
[2] M. J. Penn, B. L. Dougherty, B. Cabrera, and D. L. Sisson, Nucl. Instrum. Methods A **364**, 118 (1995).
[3] P. N. Luke, J. Appl. Phys. **64**, 6858 (1988).
[4] E. M. Conwell, Phys. Rev. A **135**, 1138 (1964).
[5] L. Pages, E. Bertel, H. Joffre, and L. Sklavenitis, At. Data **4**, 1 (1972).
[6] J. C. Ashley, C. J. Tung, R. H. Ritchie, and V. E. Anderson, IEEE Trans. Nucl. Sci. **NS-23**, 1833 (1976).
[7] G. Restelli and A. Rota, in *Semiconductor Detectors*, edited by G. Bertolini and A. Coche (North-Holland, Amsterdam, 1968).
[8] F. F. Chen, *Introduction to Plasma Physics and Controlled Fusion* (Plenum, New York, London, 1984), Vol. I.
[9] J. S. Blakemore, *Semiconductor Statistics* (Dover, New York, 1987), Chap. 6.
[10] V. N. Abakumov, V. I. Perel, and I. N. Yassievich, Sov. Phys. Semicond. **12**, 1 (1978).
[11] B. L. Dougherty, B. Cabrera, A. T. Lee, M. J. Penn, B. A. Young, and J. G. Pronko, Nucl. Instrum. Methods A **333**, 464 (1993).
[12] R. A. Smith, *Semiconductors*, 2nd ed. (Cambridge University Press, London, 1978).
[13] Assuming that the trapping cross sections are not too different in Ge, which is true for trapping on ionized impurities, then recent data in Ge are applicable. See T. Shutt, N. Wang, B. Ellman, Y. Giraud-Heraud, C. Stubbs, P. D. Barnes, Jr., A. Cummings, A. DaSilva, J. Emes, A. E. Lange, R. R. Ross, B. Sadoulet, G. Smith, W. Stockwell, S. White, B. A. Young, and D. Yvon, Phys. Rev. Lett. **69**, 3531 (1992); T. Shutt, Ph.D. thesis, University of California, Berkeley, 1993 (unpublished).
[14] S. Ramo, Proc. IRE **27**, 584 (1939).
[15] B. Cabrera (personal communication).
[16] E. Segre, *Nuclei and Particles*, 2nd ed. (Benjamin, Reading, MA, 1977).
[17] P.D. Barnes, Jr. and CDMS Collaboration, Sixth International Workshop on Low-Temperature Detectors, Beatenberg/Interlaken, Switzerland, 28 August–1 Sept. 1995 (to appear in Nucl. Instrum. Methods A).